ISSN 0022-4766, Journal of Structural Chemistry, 2022, Vol. 63, No. 11, pp. 1751-1757. © Pleiades Publishing, Ltd., 2022.
Text © The Author(s), 2022, published in Zhurnal Strukturnoi Khimii, 2022, Vol. 63, No. 11, 101100.

SYNTHESIS OF A NEW LAYERED Zn(II) COORDINATION POLYMER *VIA* DUAL-LIGAND STRATEGY: LUMINESCENCE SENSING FOR DETECTION OF Fe^{3+} ION*

Y. Tang[1] and X. Yao[2]**

A new Zn(II) coordination polymer with the formula of $[Zn(L)(4,4'\text{-Hbpt})]_n$ (**1**, H_2L = 5-[(3-carboxy-4-hydroxyphenyl)sulfanyl]-2-hydroxybenzoic acid, 4,4′-Hbpt = 1H-3,5-bis(4-pyridyl)-1,2,4-triazole) has been successfully synthesized under hydrothermal conditions. Structural characterization revealed that compound **1** displays a 2D layered structure with 4-connected **sql** topology. Interlayer N–H···O hydrogen bonds finally directed these 2D layers into an interdigitated 3D supramolecular framework. Interestingly, compound **1** shows moderate sensing ability for the recognition of Fe^{3+} ion and the minimum limit of detection (LOD) for Fe^{3+} is 0.05 mM, indicating that such layered structure can be applied as a luminescence probe for the detection of Fe^{3+} ion.

DOI: 10.1134/S002247662211004X

Keywords: Zn(II) compound, 2D layer, hydrothermal synthesis, luminescence, supramolecular framework.

INTRODUCTION

Employing multidentate organic ligands to bridge metal ions into new functional coordination polymers (FCPs) has attracted considerable interest [1-6], and these FCPs show promising potential application prospects in the realm of adsorption/separation, luminescence sensing, drug transportation, magnetism, photocatalysis and so on because of their unique structural characteristics such as high specific surface area, large pore aperture, modified functional group, etc. [7-10]. With the rapid development of economy, the global water pollution has become a serious problem that people have to cope with. The toxic pollutants, such as harmful metal ions, antibiotics, organic dyes, aromatic explosives, etc., are posing a serious threat to human health. In order to quickly detect these harmful substances, luminescent CPs are widely constructed and used as luminescence probes for the detection of pollutants mentioned above. Compared to traditional detection methods, the advantages of CPs-based luminescence probe are short response time, portable operating, visible to the naked eye, excellent sensitivity and high selectivity, and so on [11-15]. Up to now, the luminescent CPs are mainly constructed from the

[1]Analysis and Testing Center, Guangdong University of Petrochemical Technology, Guangdong, Maoming, People`s Republic of China. [2]School of Chemistry, Guangdong University of Petrochemical Technology, Guangdong, Maoming, People`s Republic of China; **xiaoqing_yao@163.com. Original article submitted July 8, 2022; revised July 26, 2022; accepted July 26, 2022.

* Supplementary materials are available for this article at doi 10.1134/S002247662211004X and are accessible for authorized users.

self-assembly of conjugated organic ligands and transition metal ions [16-18]. Therefore, selection of suitable organic ligands with large conjugated chromophores is feasible to fabricate CPs with strong luminescence [19-22]. 5-[(3-Carboxy-4-hydroxyphenyl)sulfanyl]-2-hydroxybenzoic acid (H_2L) has two carboxylate groups and can display various conformations due to the flexible –S– group, and 1H-3,5-bis(4-pyridyl)-1,2,4-triazole (4,4′-Hbpt) has five potential coordination sites and features a large conjugated chromophore (Scheme 1). The combination of H_2L and 4,4′-Hbpt, namely dual-ligand strategy, may help us to construct new CPs with intense luminescence. Therefore, in this work, we selected them as the organic building blocks to react with Zn(II) ions under hydrothermal conditions. As expected, a new Zn(II) coordination polymer formulated as $[Zn(L)(4,4'\text{-Hbpt})]_n$ (**1**) has been synthesized, which displays a 2D layered structure and emits intense luminescence. Interestingly, such luminescent coordination polymer shows moderate sensitivity toward Fe^{3+} *via* luminescence quenching, and the minimum limit of detection for Fe^{3+} is 0.05 mM.

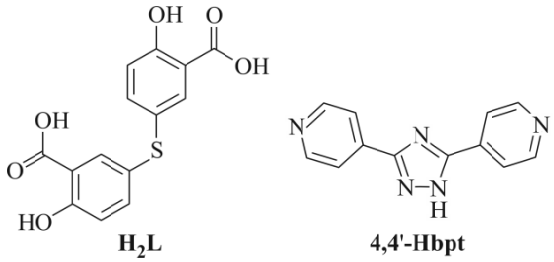

H_2L **4,4'-Hbpt**

Scheme 1. The chemical structures for the used organic ligands in this work.

EXPERIMENTAL

Materials and methods. The chemical reagents in this work were purchased and used without further purification. Elemental analysis of C, H and N was carried out on a PerkinElmer 240C elemental analyzer. Powder X-ray diffraction characterization was conducted on a Rigaku D/max-IIIA diffractometer (CuK_α, λ = 1.54056 Å) in the 2θ range of 5-50°. Thermogravimetric analysis data was collected on a Mettler Toledo TGA instrument under an air atmosphere with a heating rate of 10 °C/min in the range of 30-800 °C. Luminescent spectra data were collected on a Hitachi F-7000 luminescence spectrophotometer.

Synthesis of compound 1. (0.1 mmol, 0.029 g) $Zn(NO_3)_2{\cdot}6H_2O$, (0.1 mmol, 0.030 g) H_2L, (0.1 mmol, 0.02 g) 4,4′-Hbpt, and (0.2 mmol, 0.016 g) $NaHCO_3$ were mixed into a 12 mL H_2O. Then the mixture was transferred into a 25 mL Teflon stainless reactor and heated at 150 °C for 72 h. After that, the temperature was cooled to room temperature at a rate of 2 °C/min, colorless block crystals of **1** were obtained and washed by H_2O and further dried in air (yield: 34% based on H_2L). Elemental analysis calcd for $C_{26}H_{17}N_5O_6SZn$ (592.88) (%): C 52.62, H 2.87, N 11.81. Found (%): C 52.58, H 2.92, N 11.78.

X-ray crystallography. The crystal structure data of **1** were collected on a Rigaku Mercury CCD diffractometer equipped with a graphite-monochromated MoK_α radiation (λ = 0.71073 Å) at room temperature. The structure of **1** was solved by direct methods and refined by full-matrix least squares based on F^2 using the Olex2.0 program [23]. All non-hydrogen atoms were refined anisotropically, and all hydrogen atoms were located at their geometrical positions and refined isotropically. Crystallographic data and refinements for **1** are summarized in Table 1. Selected bond lengths and angles are list in Table S1 (Supplementary Materials) displayed in the supporting information.

Luminescence sensing experiments. 50 mg powder samples of **1** was dispersed into 5 mL different solvents and further treated ultrasonically for 30 min. The obtained suspensions were used for the next luminescence test. The luminescence sensing experiments of metal ions were carried out as follows: 50 mg powder samples of **1** were dispersed into a 5 mL EtOH solution containing $1.8{\cdot}10^{-3}$ mol/L $M(NO_3)_x$ (M^{x+} = Mg^{2+}, Ca^{2+}, La^{3+}, K^+, Na^+, Al^{3+}, Fe^{3+}), and each luminescence measurement for these suspensions was performed after 30 min of ultrasound treatment. Titration experiments

TABLE 1. Crystallographic Data and Structure Refinements for Compound **1**

Parameter	Value
Empirical formula	$C_{26}H_{17}N_5O_6SZn$
Temperature, K	293(2)
Crystal color	Colorless
Formula weight	592.88
Crystal system	Monoclinic
Space group	$P2_1/c$
a, b, c, Å	10.492(3), 20.476(5), 12.912(3)
β, deg	111.943(3)
V, Å^3	2572.9(11)
Z	4
ρ_{calcd}, g/cm^3	1.531
μ, mm^{-1}	1.087
F(000)	1208
θ Range for data collection, deg	5.856 to 54.974
Collected / unique reflections	19775 / 5784
R_{int}	0.0428
GOOF on F^2	1.047
R_1, wR_2 ($I > 2\sigma(I)$) / R_1, wR_2 (all data)	0.0420, 0.1206 / 0.0533, 0.1292
CCDC	2175782

were also performed to evaluate the sensing sensitivity of **1** toward Fe^{3+} ion by gradually adding the concentration of Fe^{3+} in EtOH solution.

RESULTS AND DISCUSSION

The single crystal structural analysis revealed that compound **1** features a 2D layered structure with 4-connected **sql** topology. Its basic building unit consists of one Zn(II) ion, one L^{2-} ligand, and one 4,4′-Hbpt ligand. As shown in Fig. 1*a*, the Zn(II) ion is surrounded by three oxygen donors and two nitrogen donors, constituting a slightly distorted trigonal bipyramidal polyhedron with the Zn–O and Zn–N distances in the range of 1.9926(18)-2.2919(19) Å, 2.060(2)-2.075(2) Å, respectively. Each L^{2-} ligand bridges two Zn(II) ion with one carboxylate group in monodentate mode and the other carboxylate group in chelating mode, and the dihedral angle between two benzene rings is 87.30°. Each 4,4′-Hbpt ligand also bridges two Zn(II) ions *via* the coordination of two pyridine nitrogen atoms, and the dihedral angles between the pyridine and triazole rings are 6.99°, 14.15°, respectively. Based on this coordination pattern of L^{2-} and 4,4′-Hbpt ligands, all Zn(II) ions were connected to form a 2D layered structure, extending along the *ac* plane (Fig. 1*b*). In this 2D layer, the Zn(II) ions and organic ligands (L^{2-} and 4,4′-Hbpt) can be topologically viewed as 4-connected nodes, and linear connectors. Thus, the structure of **1** can be simplified as a 4-connected **sql** topological network with the point symbol of $\{4^4.6^2\}$ (Fig. 1*c*). Finally, adjacent 2D layers are directed by the intermolecular N–H···O hydrogen bonds (N3–H3…O6$^{\#1}$ = 2.736 Å, ∠N3H3O6$^{\#1}$ = 166°, symmetry code: 1–*x*, 1/2+*y*, 1/2–*z*) to form an interdigitated 3D supramolecular framework (Fig. 1*d*).

The phase purity was demonstrated by the PXRD experiment. As shown in Fig. 2*a*, the experimental pattern of the bulk is highly matchable with that simulated from the single crystal diffraction data, revealing its good phase purity. Also, the thermal stability of **1** was evaluated through the TGA experiment performed in an air atmosphere from 30 °C to 800 °C. The TGA curve for **1** shown in Fig. 2*b* indicates that its struture shows no obvious change before 285 °C. The main weight loss

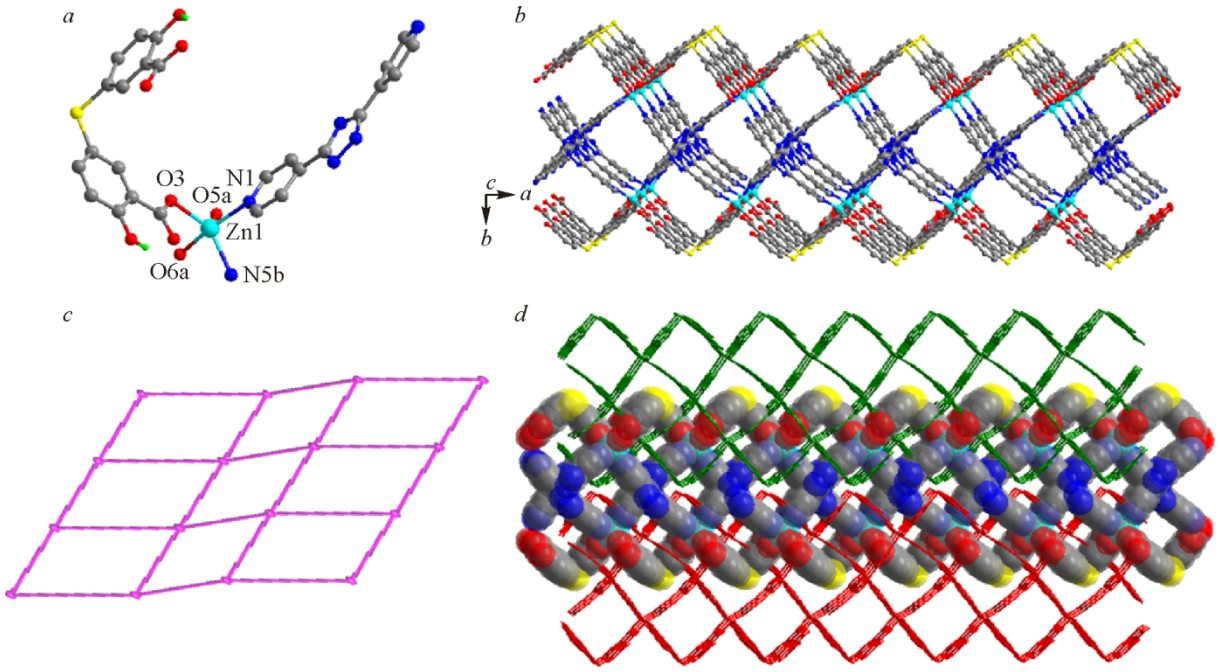

Fig. 1. The coordination environment of Zn(II) ion in **1** (*a*); the 2D layered structure of **1** (*b*); 4-connected **sql** topological net for **1** (*c*); intermolecular N–H···O hydrogen bonds directed 3D interdigitated supramolecular framework (*d*).

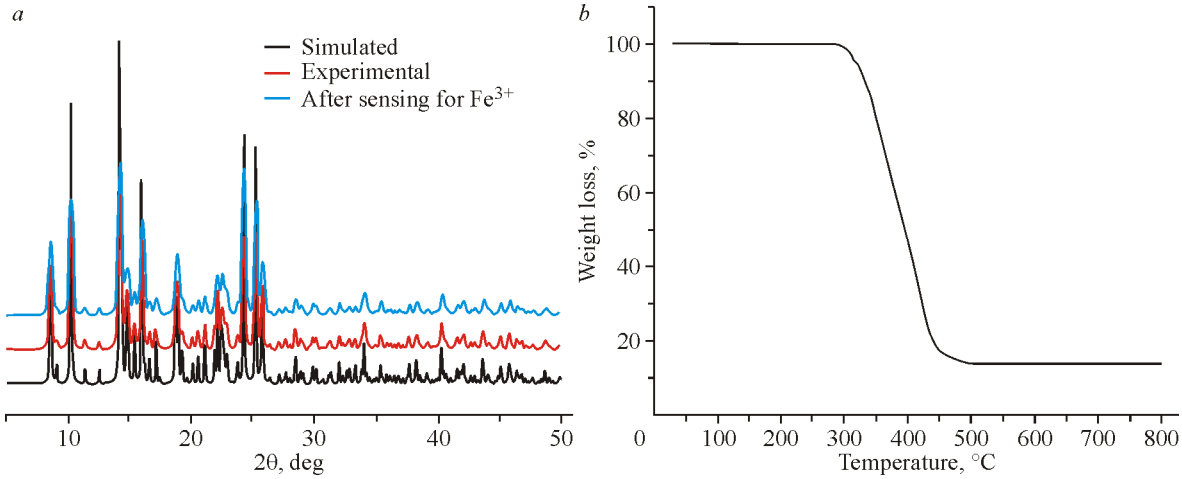

Fig. 2. The PXRD patterns for **1** (*a*); the TGA curve of **1** (*b*).

between 285 °C and 500 °C correpsonds to the combustion of the organic ligands. The final undefined residue of 13.86% may inbdicate the formation of ZnO (calcd: 13.73%).

The solid-state emission spectra of compound as well as the organic ligands were measured at room temperature. As shown in Fig. S1 (Supplementary Materials), the emission spectrum of **1** has a broad emission band with maxima at 454 nm (λ_{ex} = 380 nm), and the emission peaks for free H_2L and 4,4′-Hbpt ligands are observed at 415 nm (λ_{ex} = 360 nm), 412 nm (λ_{ex} = 370 nm), respectively, which was resulted by the intra-ligand $\pi^* \rightarrow \pi/n$ charge transfer. Notably, the maximum emission peak of **1** is red-shifted compared to those of free organic ligands. Because of the d^{10} electronic configuration, Zn(II) ion is difficult to reduce or oxidize. Thus, the luminescence emission of may originate from intra-ligand or inter-ligand $\pi^* \rightarrow \pi/n$ charge transfer [24, 25].

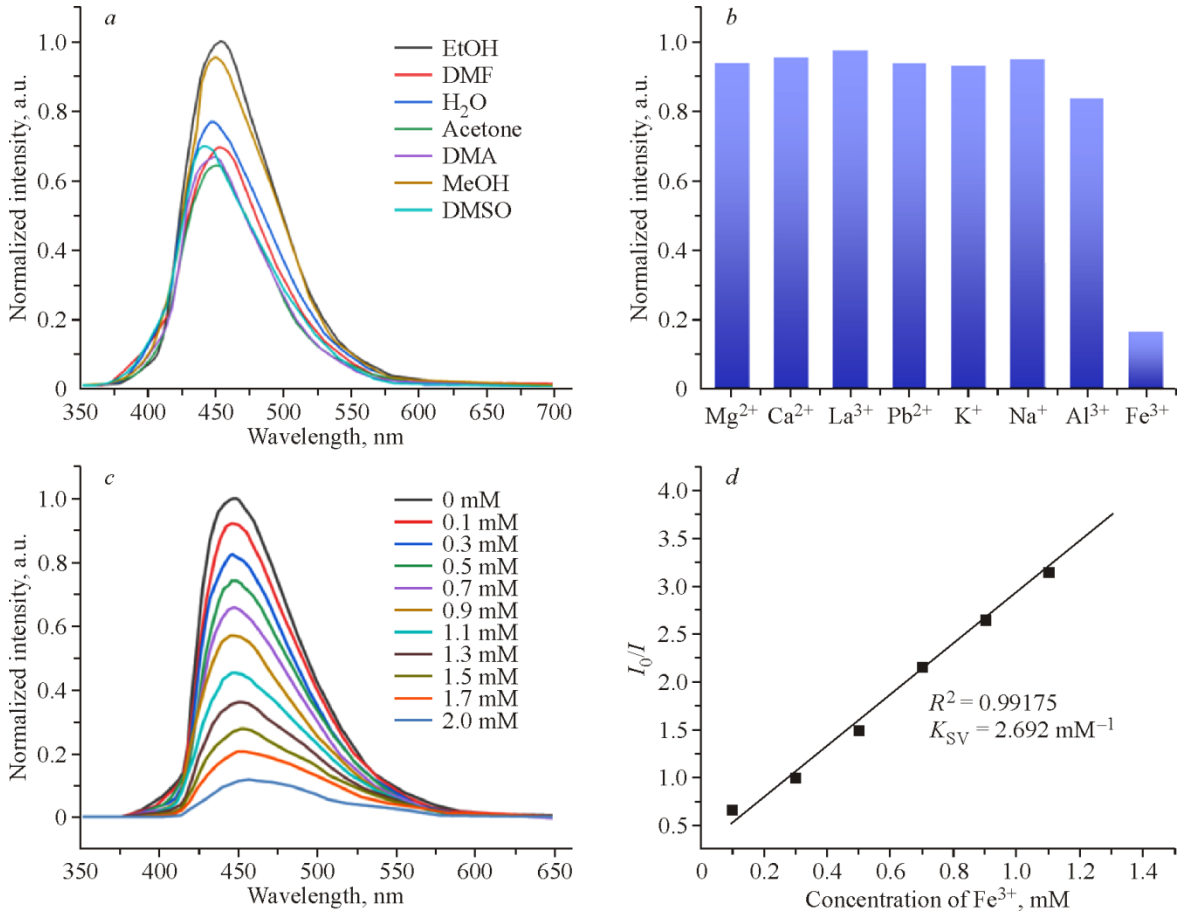

Fig. 3. The luminescence emission spectra of **1** dispersed in different solvents (*a*); luminescence emission intensity of **1** dispersed in different metal ion solutions (*b*); the change of luminescence emission spectra with the variation of Fe^{3+} concentration (*c*); Stern–Volmer plot of I_0/I versus the Fe^{3+} concentration (*d*).

The intense luminescence of **1** further inspired us to investigate its sensing properties. The luminescent spectra of compound **1** dispersed in different solvents were measured. As shown in Fig. 3*a*, the luminescent intensity of **1** depends on the identities of solvent. The intensity of **1** was strongest in EtOH solution. Thus, EtOH solvent was selected for the following investigations about sensing metal ions using **1**. The results show that Fe^{3+} ion can quench the luminescence of **1** significantly while other metal ions, such as Mg^{2+}, Ca^{2+}, La^{3+}, Pb^{2+}, K^+, Na^+, Al^{3+}, have negligible effect on the luminescence intensity of **1** (Fig. 3*b*), indicating that compound **1** may have potential as a luminescent probe for the detection of Fe^{3+} *via* luminescence quenching. The sensing sensitivity toward Fe^{3+} ion was further evaluated *via* the titration experiment by gradually adding the concentration of Fe^{3+}. As shown in Fig. 3*c*, the emission intensity of **1** decreased sequentially with the evaluation of Fe^{3+} concentration. According to the reports, the quenching efficiency by Fe^{3+} ion can be quantitively expressed *via* the quenching constant. Based on the Stern–Volmer equation of $I_0/I = 1 + K_{sv}$ [Fe^{3+}] (I_0: luminescence intensity without adding Fe^{3+}, I: luminescence intensity after adding Fe^{3+}, K_{sv}: quenching constant, [Fe^{3+}]: Fe^{3+} concentration), the quenching constant (K_{sv}) can be calculated to be 2.692 mM^{-1} (Fig. 3*d*). The minimum limit of detection (LOD) was also calculated according to the equation: of LOD = 3σ/*k* (σ: the standard deviation, *k*: the slope of the Stern–Volmer equation), giving rise to a value of 0.05 mM. These results are comparable to those of reported MOFs [26, 27], indicating that compound **1** is a good candidate as luminescence probe for the detection of Fe^{3+}. After the luminescence sensing for Fe^{3+} ion, the structure of **1** shows no obvious change that ruled out luminescence quenching caused by the structure collapse (Fig. 2*a*). After sensing experiment for Fe^{3+} ion, the solids of **1** were filtered and further washed by 100 mL H_2O for six times. The solids after dried in a 100 °C oven for 10 h were further analyzed by the inductively coupled plasma emission spectroscopy (ICP), founding

that such solids contain 5.6% Fe element. Thus, the possible quenching mechanism by Fe^{3+} ions may be caused by the coordination of uncoordinated nitrogen atoms with Fe^{3+} ions, which can promote electron transfer effectively from organic ligand to Fe^{3+} ion.

In summary, the synergistic coordination of L^{2-} and 4,4′-Hbpt with Zn(II) ions under hydrothermal conditions afforded a new 2D layered Zn(II) coordination polymer. Such compound displays intense luminescence, and shows moderate sensitivity toward Fe^{3+} ion, indicating that it may be served as a luminescence probe for the detection of Fe^{3+} ion.

ACKNOWLEDGMENTS

This work was supported by Guangdong University of Petrochemical Technology.

CONFLICT OF INTERESTS

The authors declare that they have no conflicts of interests.

REFERENCES

1. H.-Y. Li, S.-N. Zhao, S.-Q. Zang, and J. Li. *Chem. Soc. Rev.*, **2020**, *49*(17), 6364-6401. https://doi.org/10.1039/c9cs00778d
2. A. Kuznetsova, V. Matveevskaya, D. Pavlov, A. Yakunenkov, and A. Potapov. *Materials (Basel)*, **2020**, *13*(12), 2699. https://doi.org/10.3390/ma13122699
3. K. A. Kovalenko, A. S. Potapov, and V. P. Fedin. *Russ. Chem. Rev.*, **2022**, *91*(4), RCR5026. https://doi.org/10.1070/rcr5026
4. M. I. Rogovoy, A. S. Berezin, Y. N. Kozlova, D. G. Samsonenko, and A. V. Artem′ev. *Inorg. Chem. Commun.*, **2019**, *108*, 107513. https://doi.org/10.1016/j.inoche.2019.107513
5. M. I. Rogovoy, D. G. Samsonenko, M. I. Rakhmanova, and A. V. Artem′ev. *Inorg. Chim. Acta*, **2019**, *489*, 19-26. https://doi.org/10.1016/j.ica.2019.01.036
6. A. V. Artem′ev, M. P. Davydova, X. Hei, M. I. Rakhmanova, D. G. Samsonenko, I. Y. Bagryanskaya, K. A. Brylev, V. P. Fedin, J.-S. Chen, M. Cotlet, and J. Li. *Chem. Mater.*, **2020**, *32*(24), 10708-10718. https://doi.org/10.1021/acs.chemmater.0c03984
7. D. I. Pavlov, A. A. Ryadun, and A. S. Potapov. *Molecules*, **2021**, *26*(23), 7392. https://doi.org/10.3390/molecules26237392
8. Y.-N. Wang, S.-D. Wang, J.-H. Lv, K.-Z. Cao, H.-Q. Liu, F. Wang, and S.-Q. Lu. *J. Mol. Struct.*, **2022**, *1247*, 131317. https://doi.org/10.1016/j.molstruc.2021.131317
9. L. Guo, Y. Liu, L. Guo, J. Cao, W. Li, T. Liu, S. Qiao, and B. Wang. *Z. Anorg. Allg. Chem.*, **2021**, *647*(10), 1077-1082. https://doi.org/10.1002/zaac.202000367
10. J. Luo, F. Jiang, R. Wang, L. Han, Z. Lin, R. Cao, and M. Hong. *J. Mol. Struct.*, **2004**, *707*(1-3), 211-216. https://doi.org/10.1016/j.molstruc.2004.07.029
11. P. Wu, Y. Liu, Y. Liu, J. Wang, Y. Li, W. Liu, and J. Wang. *Inorg. Chem.*, **2015**, *54*(23), 11046-11048. https://doi.org/10.1021/acs.inorgchem.5b01758
12. Y.-X. Sun, G. Guo, W.-M. Ding, W.-Y. Han, J. Li, and Z.-P. Deng. *CrystEngComm*, **2022**, *24*(7), 1358-1367. https://doi.org/10.1039/d1ce01432c
13. Z.-F. Wu, L.-K. Gong, and X.-Y. Huang. *Inorg. Chem.*, **2017**, *56*(13), 7397-7403. https://doi.org/10.1021/acs.inorgchem.7b00505
14. H.-N. Wang, P.-X. Liu, H. Chen, N. Xu, Z.-Y. Zhou, and S.-P. Zhuo. *RSC Adv.*, **2015**, *5*(80), 65110-65113. https://doi.org/10.1039/c5ra10336c

15. N.-N. Zeng, L. Ren, and G.-H. Cui. *CrystEngComm*, **2022**, *24*(5), 931-935. https://doi.org/10.1039/d1ce01537k
16. D. I. Pavlov, T. S. Sukhikh, A. A. Ryadun, V. V. Matveevskaya, K. A. Kovalenko, E. Benassi, V. P. Fedin, and A. S. Potapov. *J. Mater. Chem. C*, **2022**, *10*(14), 5567-5575. https://doi.org/10.1039/d1tc05488k
17. Y.-Q. Su, Y.-H. Qu, L. Fu, and G.-H. Cui. *Inorg. Chem. Commun.*, **2020**, *118*, 108013. https://doi.org/10.1016/j.inoche.2020.108013
18. J. Yin, Y. Han, H. Zhu, and Y. Tian. *J. Chem. Res.*, **2021**, *45*(9/10), 845-849. https://doi.org/10.1177/1747519821101898 1
19. X.-J. Wei, D. Liu, Y.-H. Li, and G.-H. Cui. *J. Solid State Chem.*, **2020**, *284*, 121218. https://doi.org/10.1016/j.jssc.2020.121218
20. C. Xu, L. Li, Y. Wang, Q. Guo, X. Wang, H. Hou, and Y. Fan. *Cryst. Growth Des.*, **2011**, *11*(10), 4667-4675. https://doi.org/10.1021/cg200961a
21. R.-P. Ye, J.-X. Yang, X. Zhang, L. Zhang, and Y.-G. Yao. *J. Mol. Struct.*, **2016**, *1106*, 192-199. https://doi.org/10.1016/j.molstruc.2015.10.086
22. Y. Bu, F. Jiang, K. Zhou, X. Li, L. Zhang, Y. Gai, and M. Hong. *CrystEngComm*, **2013**, *15*(42), 8426. https://doi.org/10.1039/c3ce41417e
23. G. M. Sheldrick. *Acta Crystallogr*., *Sect. C: Struct. Chem.*, **2015**, *71*(1), 3-8. https://doi.org/10.1107/s2053229614024218
24. J.-X. Yang, X. Zhang, J.-K. Cheng, J. Zhang, and Y.-G. Yao. *Cryst. Growth Des.*, **2012**, *12*(1), 333-345. https://doi.org/10.1021/cg201143f
25. H. Zhu, L. Fu, D. Liu, Y.-H. Li, and G.-Y. Dong. *J. Solid State Chem.*, **2020**, *286*, 121265. https://doi.org/10.1016/j.jssc.2020.121265
26. C. Bai, F.-H. Wei, H.-M. Hu, L. Yan, X. Wang, and G.-L. Xue. *J. Lumin.*, **2020**, *227*, 117545. https://doi.org/10.1016/j.jlumin.2020.117545
27. R. Goswami, S. C. Mandal, B. Pathak, and S. Neogi. *ACS Appl. Mater. Interfaces*, **2019**, *11*(9), 9042-9053. https://doi.org/10.1021/acsami.8b20013